Nernst-Planck-Poisson Model for the Description of Behaviour of Solid-Contact Ion-Selective Electrodes at Low Analyte Concentration

Jerzy J. Jasielec,[a] *Grzegorz Lisak*,[a] *Michal Wagner*,[a] *Tomasz Sokalski*,[a] *Andrzej Lewenstam**[a, b]

[a] Process Chemistry Centre, c/o Centre for Process Analytical Chemistry and Sensor Technology (ProSens), Åbo Akademi University, Biskopsgatan 8, 20500 Åbo-Turku, Finland
[b] AGH – University of Science and Technology, Faculty of Material Science and Ceramics, Al. Mickiewicza 30, 30059 Cracow, Poland
*e-mail: andrzej.lewenstam@abo.fi

Received: July 12, 2012
Accepted: October 10, 2012
Published online: December 5, 2012

Abstract
All-solid-state electrodes are increasingly being used in clinical, industrial and environmental analysis. This wide range of applications requires deep theoretical description of such electrodes. This work concentrates on the development of a numerical tool for the qualitative prediction of electrochemical behaviour for solid-contact ion-selective electrodes at low analyte concentrations. For this purpose, a general approach to the description of electro-diffusion processes, namely the Nernst-Planck-Poisson (NPP) model, was applied. The results obtained from this model are verified by experimental data of lead(II)-selective electrodes based on a polymeric PVC membrane with polybenzopyrene doped with Eriochrome Black T used as the solid contact.

Keywords: Potentiometry, Ion-selective electrodes, Solid contact, Response, Nernst-Planck-Poisson model, Electrodiffusion

DOI: 10.1002/elan.201200353

1 Introduction

Owing to several advantages, potentiometric sensors are broadly used in clinical and environmental analysis. Instrumentation and sensors are relatively cheaper and more user-friendly than other analytical techniques. Moreover, the potentiometric measurements do not change the sample's chemical composition [1].

The aspect of lowering of the detection limit of ion-selective electrodes (ISEs) has been an issue of interest for all types of potentiometric sensors. The first trials were performed with solid-state membrane electrodes [2–4]. Later, electrodes with polymeric membranes and inner filling solution were used [5,6]. More recently, solid-contact ion-selective electrodes (SC ISEs) with polymer membranes were applied [7–10]. In the latter electrodes, the inner filling solution is deliberately replaced with an intermediate layer between electrically conducting substrate and the solvent polymeric membrane [11]. The materials frequently used for this purpose are conducting polymers (CPs). Owing to their mixed conductivity, CPs serve as the elements that unblock faradaic charge transfer at the contact interfaces and thus adequately act as ion-to-electron transducers [12–14]. Applications of various conducting polymers as the SCs are extensively presented in the literature. Among them the most popular are: polypyrrole (PPy), poly(3-octyltiophene) (PEDOT) and polyaniline (PANI) [15]. In respect of lowering the detection limit, the removal of inner filling solution may bring advantages in reducing transmembrane ion fluxes from the inner compartment to the sample solution as well as allowing miniaturization [7,16].

Much effort is being put into developing a sensor which would operate at nanomolar concentrations. In particular, the determination of heavy metals is one of the major interests [17–19].

Understanding the processes involved in the response of ISEs at low analyte concentration is crucial in environmental analysis. Theoretical modelling brings new insight into those processes. Ideally, a tool which would predict the behaviour of a particular system is needed.

There are many models describing the response of ISEs, but they differ in generality and idealization level. Among them, the Nernst-Planck-Poisson (NPP) model offers the most complete and universal description of membranes and related systems [1].

Since the first application of the NPP model to membrane electrochemistry was presented in 1978 [20], an approach dedicated to the general description of ISE behaviour was developed [21–25]. In the mentioned papers, the authors describe the ISE potential as the effects of diffusion and migration taking place only in an ion-selective membrane.

The extension of the NPP model to a two-layer system made it possible to simulate the processes occurring in

the diffusion layer, and as a result to show the effects of low detection limit (LDL) [26]. All the mentioned papers provide descriptions of the classical electrodes containing inner filling solution.

Currently the increased usage of solid-contact ion-selective electrodes creates the necessity of a proper theoretical description of such systems. This work is the first attempt at such a description to be presented in the literature.

2 Theoretical Description of ISE

2.1 Available Models

The models used for the description of ISEs may be roughly divided into three categories: 1) phase boundary models, 2) diffusion layer models, and 3) models including migration. They can also be divided into time-dependent and time-independent (equilibrium and steady-state) models [1,27].

The simplest models, such as the Nikolskii-Eisenman equation are insufficient to describe the presented system, and therefore more advanced modelling has to be used. In our recent work [26] all models suitable for the proper description of the time-dependent potential formation of the classical electrodes at low analyte concentration have been presented.

The case considered in this work is more complicated, as not only concentration and electrical field profiles inside the membrane and the diffusion layer determine the resulting potential, but also the properties of CP (as a separate phase) and concentration/field changes inside it have to be taken into account.

The complexity of presented system requires advance modelling, and makes the usage of the simple models (still applicable for classical ISE) impossible. Therefore, a multi-layer NPP model has to be applied.

2.2 Multilayer NPP Model

In the case of ISE using the CP, the time-dependent potential is the effect of concentration/field changes inside the diffusion layer, ion-selective membrane and conductive polymer.

Even though the NPP model for an arbitrary number of layers was developed and implemented in C++ [28], as well as in MathCad [29] and Matlab [30] scripts, no systems with more than 2 layers have been analyzed so far.

In this work we consider the system which consists of three layers – the first representing the diffusion layer of aqueous solution, the second representing the ion-selective membrane and the third that represents the conducting polymer. Each layer has its own thickness d^j and dielectric permittivity ε^j, is flat and isotropic, so it can be considered as a continuous environment inside which the change in time and space of the concentration of r components c_i^j and of electric field E^j takes place. This system is presented in Figure 1.

The NPP model is an initial-boundary value problem, which for one dimension is given by the set of equations shown below.

The ionic fluxes are expressed by the Nernst-Planck equation:

$$J_i^j(t,x) = -D_i^j\left[\frac{\partial c_i^j(t,x)}{\partial x} + \frac{F}{RT} z_i c_i^j(t,x) E^j(t,x)\right] \tag{1}$$

where: $J_i^j(t,x)$ is the flux of the i-th ion in the j-th layer, D_i^j is the constant self-diffusion coefficient of the i-th ion in the j-th layer, $c_i^j(t,x)$ is the concentration of i-th ion in the j-th layer, z_i the valence of i-th ion, and $E^j(t,x)$ is the electric field in the j-th layer. F is the Faraday constant, R and T denote the gas constant and absolute temperature.

The mass conservation law describes the evolution of concentrations:

$$\frac{\partial c_i^j(t,x)}{\partial t} = -\frac{\partial J_i^j(t,x)}{\partial x} \tag{2}$$

In this work, the Poisson equation is replaced by its equivalent form, the total current equation:

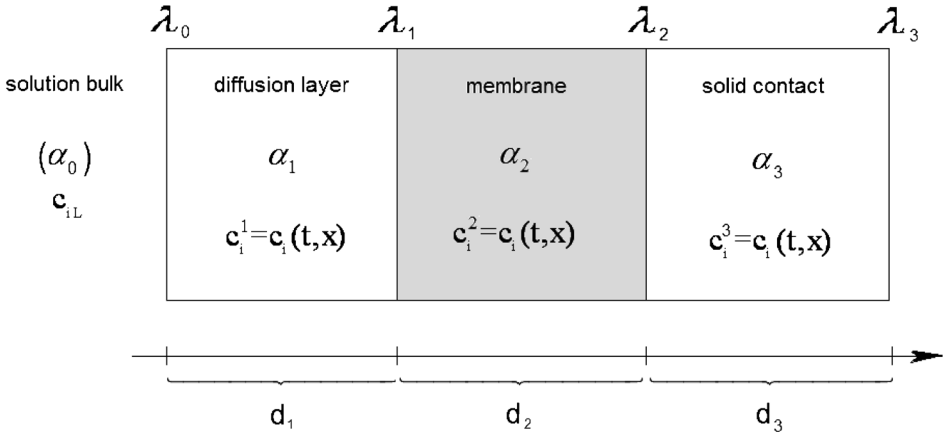

Fig. 1. Scheme of a 3-layer system, where α_1 represents the diffusion layer in external solution (sample), α_2 is the ion-selective membrane and α_3 is the solid contact (here: conductive polymer). c_{iL} is the constant concentration of the i-th component in the bulk of the sample solution.

$$I(t) = F\sum_{i}^{n} z_i J_i^j(t,x) + \varepsilon^j \frac{\partial E^j(t,x)}{\partial t} \quad (3)$$

The values of fluxes at the boundaries (the interface λ_j between layers α_j and α_{j+1}) are calculated using Neumann-like boundary conditions, namely modified Chang–Jaffe conditions in the form:

$$J_i^j(\lambda_j,t) = J_i^{j+1}(\lambda_j,t) = \overrightarrow{k_{i\lambda_j}} c_i^j(\lambda_j,t) - \overleftarrow{k_{i\lambda_j}} c_i^{j+1}(\lambda_j,t) \quad (4)$$

where $\overrightarrow{k_{i\lambda_j}}$, $\overleftarrow{k_{i\lambda_j}}$ are the first-order heterogeneous rate constants used to describe the interfacial kinetics. The $\overrightarrow{k_{i\lambda_j}}$ constant corresponds to the ion i, which moves from layer α_j to α_{j+1}, and $\overleftarrow{k_{i\lambda_j}}$ – to the ion i, which moves from α_{j+1} to α_j.

Initial concentrations fulfil the electroneutrality condition and, consequently, there is no initial space charge in the system:

$$c_i^j(0,x) = c_{Mi}^j(x), \quad E^j(0,x) = 0 \quad \text{for} \quad x \in \left[0, \sum_{j=1}^{3} d_j\right] \quad (5)$$

The membrane potential, $\phi(t)$, is obviously given by:

$$\phi(t) = -\int_0^{d_1} E^1(t,x)dx - \int_{d_1}^{d_2} E^2(t,x)dx - \int_{d_2}^{d_3} E^3(t,x)dx \quad (6)$$

2.3 Numerical Experiment

The numerical experiment was performed in order to describe the conditions used also in the experimental part, and consists of the following steps:

1) conditioning of the electrode in 10^{-3} mol dm^{-3} solution of $Pb(NO_3)_2$ for 20 minutes,
2) making a calibration curve in 10^{-3} mol dm^{-3} down to 10^{-10} mol dm^{-3} solutions of $Pb(NO_3)_2$,
3) repeating steps 1 and 2.

The numerical experiment was performed for three layers. The first layer, with a thickness $d_1 = 100$ μm, represents the water diffusion layer in sample solution, the second ($d_2 = 35$ μm) represents the membrane, and the third one ($d_2 = 2$ μm) represents the conducting polymer. The dielectric permittivities were assumed to be $\varepsilon_1 = 7.08\times10^{-10}$ F m^{-1} and $\varepsilon_2 = \varepsilon_3 = 2.12\times10^{-10}$ F m^{-1}, respectively. The temperature was set to $T = 298.16$ K and the measurement time was set to 300 s for each point of the calibration curve.

NPP simulations were performed for a system containing five different ions, using the parameters shown in Table 1. The number of discretization points was set to $N_1 = 60$, $N_2 = 100$, and $N_3 = 60$ and the first step of space discretization was set to 10^{-11} m.

The calculations were made on an IBM PC with an Intel Core2 Duo (2.2 GHz) processor and 4 GB RAM under Windows XP SP3.

3 Experimental

3.1 Reagents

Lead(II) nitrate ($Pb(NO_3)_2$), lead ionophore IV, sodium tetrakis(4-fluorophenyl)borate (NaTFPB), tetrahydrofuran (THF), and poly(vinyl chloride) (PVC) high molecular weight were obtained from Fluka (Buchs, Switzerland). Potassium nitrate (KNO_3) and eriochrome black T (EbT) were obtained from Merck (Darmstadt, Germany). Benzo(a)pyrene, tetracyanoquinodimethane and acetonitrile (ACN) were obtained from Sigma-Aldrich (Steinheim,

Table 1. Ion properties used for calculations (concentrations in mol dm^{-3} and all other values in SI units). R^- is used to represent three different ions (as they do not move between phases): NO_3^- in α_1, anionic site in α_2, and eriochrome black T in α_3. X^{2+} represents various bivalent impurities.

i	z_i	D_i^1 ($\times10^{-9}$)	D_i^2 ($\times10^{-12}$) [a]	D_i^3 ($\times10^{-14}$) [a]	c_{iL}	$c_{iM}{}^1$	$c_{iM}{}^2$	$c_{iM}{}^3$	c_{iR}
Pb^{2+}	+2	0.46	1.0	1.0	[b]	10^{-3}	0	0	0
Na^+	+1	1.33	1.0	1.0	10^{-7}	10^{-7}	1.6×10^{-3}	0	0
NO_3^-	−1	1.90	1.0	1.0	2 [b]	2×10^{-3}	0	0	0
R^-	−1	5.03	1.0	1.0	0	0	1.6×10^{-3}	0	0
X^{2+}	+2	0.79	1.0	1.0	10^{-9}	10^{-9}	0	0	0

i	$\vec{k}_{i\lambda_0}$	$\vec{k}_{i\lambda_1}$	$\vec{k}_{i\lambda_2}$	$\vec{k}_{i\lambda_3}$	$\overleftarrow{k}_{i\lambda_0}$	$\overleftarrow{k}_{i\lambda_1}$	$\overleftarrow{k}_{i\lambda_2}$	$\overleftarrow{k}_{i\lambda_3}$
Pb^{2+}	0.01	0.01	0.01	0	0.01	0.01	0.01	0
Na^+	0.01	10^{-6}	0.01	0	0.01	0.01	10^{-6}	0
NO_3^-	0.01	10^{-6}	0.01	0	0.01	0.01	10^{-6}	0
R^-	0	0	0	0	0	0	0	0
X^{2+}	0.01	10^{-6}	0.01	0	0.01	0.01	10^{-6}	0

[a] Typical order of magnitude for diffusion coefficients for the membrane [e.g. 31] and for conducting polymer [e.g. 32] are used. [b] calibration curves made for 10^{-3} down to 10^{-10} mol dm^{-3}.

Germany). The chemicals were of analytical grade. Aqueous solutions were prepared with freshly deionized water (18.2 MΩ cm) obtained with the ELGA purelab ultra water system (High Wycombe, United Kingdom).

3.2 Preparation of Conducting Polymer

The polybenzopyrene (PBP) films were made by potential cycling using an Autolab PGSTAT 100 instrument controlled by General Purpose Electrochemical System (GPES) software. In the three-electrode system, the glassy carbon was the working electrode (WE), coiled platinum wire was the counter electrode (CE), and a silver wire coated with AgCl was used as the quasi-reference electrode (RE). The reference electrode was calibrated with tetracyanoquinodimethane in ACN ($E_{redox}=-0.032$ V). The surface of the WE was finally polished before using with Al_2O_3 powder (0.03 μm). Electrosynthesis of the PBP films was conducted in 10 mM EbT-ACN solution with 8 mM monomer concentration at 20 $mV\,s^{-1}$ scan rate in the potential range from 0 to 1.4 V. All studied electrodes were made within 15 potential cycles. After deposition of polybenzopyrene, the films were washed with deionized water and left for the residual water to evaporate.

3.3 Preparation of ISE

The PVC-based membranes contained 0.4 % lead ionphore IV, 0.15 % NaTFPB, 62.3 % o-NPOE, nad 37.15 % PVC (weight %). A total of 200 mg of membrane components were dissolved in 2 mL of THF. When the surface of the polybenzopyrene-based electrodes was visually waterless, the membrane cocktail was applied. Portions of 10 μL of the membrane components were applied with 10 minutes′ time delay (longer if necessary, until the visual evaporation of the solvent). The final volume was 30 μL. Subsequently, the electrodes were left for overnight evaporation of the residual solvent.

3.4 Potentiometric Measurements

A solid-contact Pb^{2+} selective electrode based on polybenzopyrene doped with Eriochrome Black T/PVC membrane served as the indicator electrode. A double-junction electrode, Orion (Thermo Scientific–Environmental Instruments, Beverly, MA, USA) with 10^{-3} $mol\,dm^{-3}$ KNO_3 | 1 mol dm^{-3} KCl served as a reference electrode. Potentiometric measurements were carried out in 100 ml disposable polystyrene beakers. Each beaker was soaked in 10^{-1} $mol\,dm^{-3}$ HNO_3 for two days and was washed with deionized water. Before the potentiometric measurement, the electrode was kept dry. Then, just before the start of the measurement the electrode was preconditioned in 50 mL of 10^{-3} $mol\,dm^{-3}$ $Pb(NO_3)_2$ for 20 minutes. Subsequently, the calibration of Pb^{2+}-selective ISE was done by automatic dilution using two Metrohm Dosino 700 instruments equipped with burets of 50 mL capacity (Metrohm, Herisau, Switzerland). The pumps were programmed to dilute the sample solution with freshly deionized water (18.2 MΩ·cm) every 5 minutes. Between the measurements, the electrode was washed with deionized water and kept dry in a closed container. The obtained data was recorded with an EMF16 Interface from Lawson Labs Inc., (Malvern, PA, USA). All experiments were performed at room temperature (20 −21 °C). The activity coefficients were calculated according to the Debye–Hückel approximation. All the EMF data were corrected for liquid-junction potentials according to the Henderson equation.

4 Results and Discussion

Conducting polymer film made of polybenzopyrene doped with Eriochrome Black T (EbT) can serve as lead(II)-sensitive film [33]. By applying a PVC-based membrane on the top of Eriochrome Black T film the enhancement in selectivity toward Pb^{2+} was achieved [34]. The presence of lead(II) complexing EbT in the CP film ($\log K_{PbL}=13.19$ for Pb(EbT) [35]) gives additional driving force for the uptake of Pb^{2+} ions from the solution through the PVC membrane into the conducting polymer film.

4.1 Numerical Results

It could be expected that the conditioning in the solution containing Pb^{2+} would result in the influx of these ions to the conductive polymer. This process would exert a significant influence on the properties of the electrode and its response, especially the detection limit.

After the first conditioning, only a small amount of Pb^{2+} is present in the conductive polymer phase. The concentration of Pb^{2+}, which enters the CP (calculated as $\int_{d_2}^{d_3} c(t,x)dx$ divided by layer width) during the first conditioning, was calculated to be 1.58×10^{-10} $mol\,dm^{-3}$. In this case, super-Nernstian response is observed (bottom curve in Figure 2). This situation is analogous to the case of classical electrodes with the low concentration of main ion in the inner solution [5,26].

After the second conditioning, more Pb^{2+} is present in the CP phase, which leads to an almost ideal Nernstian response with very low detection limit. The concentration of Pb^{2+} in the CP after the second conditioning was calculated to be 1.27×10^{-7} $mol\,dm^{-3}$. This is analogous to the case of the classical electrode with optimal main ion concentration in the inner solution.

After the third conditioning, even more Pb^{2+} is present in the CP phase, which leads to a deterioration of the Nernstian response. The concentration of Pb^{2+} in the CP after the third conditioning was calculated to be 2.10×10^{-6} $mol\,dm^{-3}$. This is analogous to the case of the classical electrode with a high main ion concentration in the inner solution.

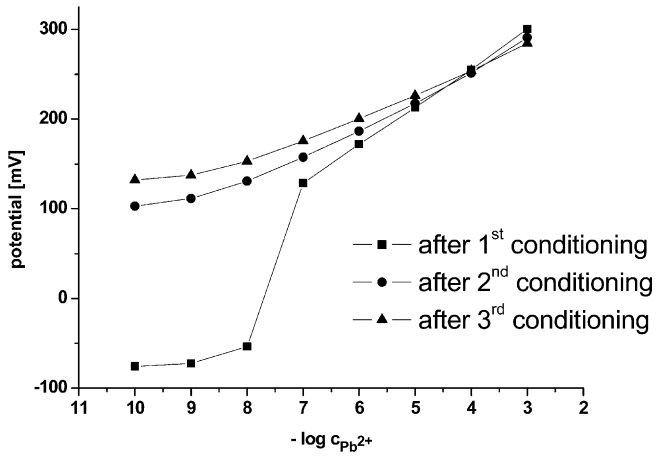

Fig. 2. Calibration curves for ISE, with CP as the solid contact, obtained from the numerical experiment.

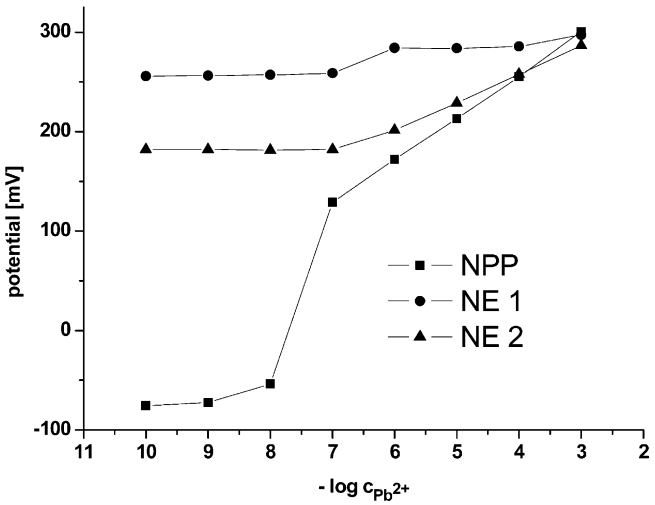

Fig. 4. Calibration curves for ISE after the first conditioning. Comparison between the NPP model and NE equation.

The increase in the concentrations of all the ions inside the conducting polymer is shown in Figure 3.

An interesting comparison between the NPP model and Nikolskii–Eisenman (NE) equation is presented in Figure 4. The concentrations obtained from NPP were used in the NE equation in two different ways: NE1) concentrations at the membrane boundaries, NE2) $\int_0^{d_1} c(t,x)dx$ divided by the diffusion layer width and $\int_{d_2}^{d_3} c(t,x)dx$ divided by the width of the conducting polymer.

The Nikolskii–Eisenman equation belongs to total equilibrium models. They are far more idealized and less general than the NPP Model (as described in detail in [1]). As has already been said by Nikolskii, his model "involves some difficulties, for in this case one deals with thermodynamically undefined variables, interface potential differences, diffusion potentials, and activities of single ions" [36]. Therefore, potential calculated using the NE equation, even based on concentrations obtained from NPP model, does not correspond well to both calculated by NPP and measured experimentally (Figure 6) especially in the low detection limit regime.

Although the experimental measurement was, for simplicity, performed in the absence of interfering ion, the influence of the interfering ion concentration is of interest for real sample measurement. The numerical experiment has been repeated with different values of the concentration of X^{2+} as an interfering ion. As shown in Figure 5, the increase in the concentration of interfering ion has the influence on the calibration curve obtained after the first conditioning, causing the decrease of super-Nernstian jump without the influence on the detection limit. For the curves obtained after the second and the third conditioning it worsens the detection limit. Further increase of the value of the interfering ion concentration, after the disappearance of super-Nernstian response, causes the deterioration of the detection limit for all three curves.

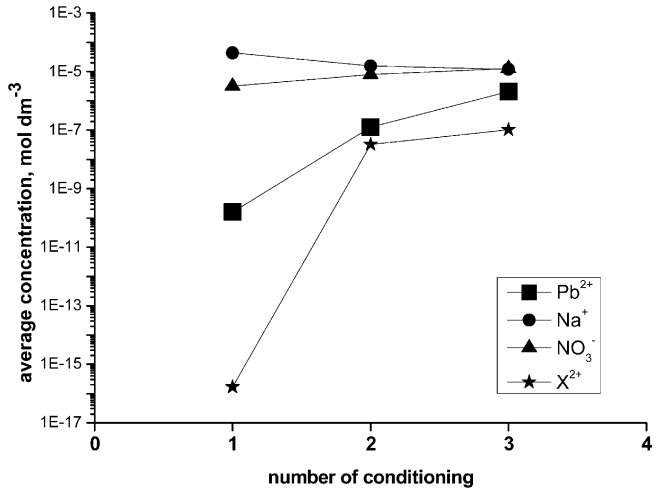

Fig. 3. The average concentrations of ions in the polymer matrix (calculated as $\int_{d_2}^{d_3} c(t,x)dx$ divided by layer width).

4.2 Experimental Results

The analytical response of SC Pb^{2+}-ISE is presented in Figure 4. Before the calibration, the electrode was preconditioned in 10^{-3} mol dm^{-3} of primary ion ($Pb(NO_3)_2$) for 20 minutes. The preconditioning took place before every calibration, while in between the electrodes were kept dry. In this way, all changes in the response of the electrodes may be attributed to the conditioning and calibration. The first calibration shows a linear response down to approximately 10^{-7} mol dm^{-3} Pb^{2+} with a slope of 30.2 mV dec^{-1}. Between 10^{-7} and 10^{-8} mol dm^{-3} Pb^{2+} a super-Nernstian response occurred. After another two conditioning procedures the super-Nernstian response disappeared (LDL ~ 10^{-7} mol dm^{-3} Pb^{2+}) with Nernstian slope attained (around 28.5–30.5 mV dec^{-1}). From the obtained results it can be concluded that the conditioning strongly affects the detection limit, while the Nernstian response within the linear part of each calibration curve is not affected. It is worth mentioning that, since the ion-

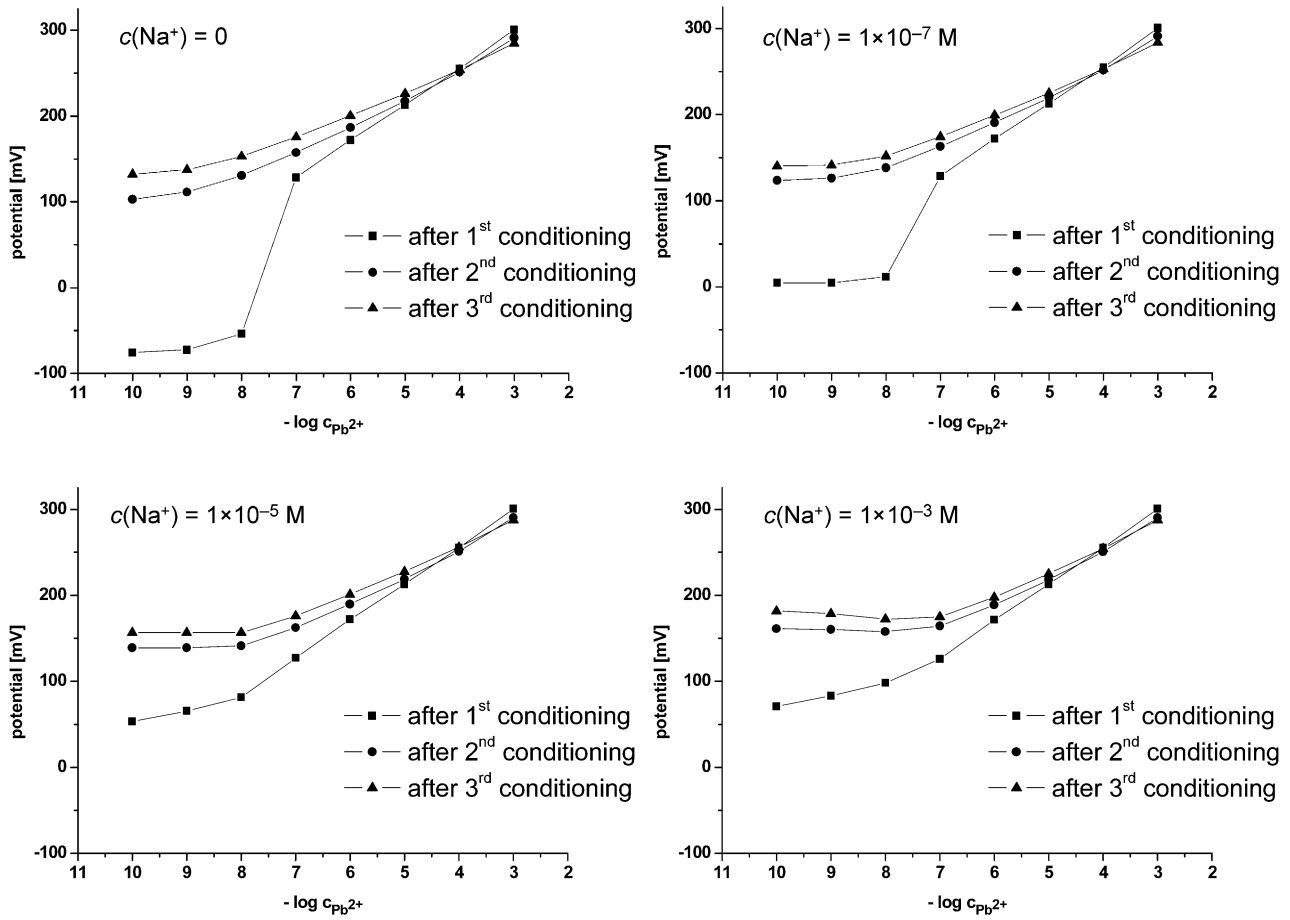

Fig. 5. Calibration curves for ISE, with CP as the solid contact, obtained from the numerical experiment with different values of interfering ion concentration, indicated in the left upper corner of each plot.

selective membranes are unconditioned the E° is constantly changing (for comparison all the curves were brought to one potential at 10^{-3} mol dm^{-3} Pb^{2+}). A short conditioning was deliberately applied to show the differences in response of the ion-selective membranes at unconditioned and well-conditioned states. When electrodes have not been sufficiently long in contact with the primary ion, the detection limit is lower due to the gradient of Pb^{2+} from the solution to unconditioned membrane. As soon as the membranes get saturated the typical detection limit is observed.

4.3 Comparison of the Results

The preparation of the ISE with CP has to be followed by the conditioning process. During conditioning in the solution of primary ion, this ion is transported through the ion-selective membrane and accumulated in the polymer matrix. The amount of the ion accumulated inside the CP strongly depends, among other parameters, on the time of the conditioning.

The potentiometric response of the ISE depends on the amount of primary ion accumulated in the CP in the same way as the response of classical electrode depends on the amount of primary ion in the inner filling solution.

After the short time of conditioning, a small amount of primary ion is accumulated in the CP matrix, which leads to a super-Nernstian response of ISE. After longer conditioning, the amount of ion accumulated in the matrix is higher and this leads to the classical type of response.

The theoretical (Figure 2) and experimental (Figure 6) results show the qualitative agreement. The CP enrichment process is shown by the theory and indicated by the experiment. The time of conditioning is the parameter which obviously has the biggest influence on this process, and therefore on the amount of primary ion accumulated in the CP matrix.

Both the theoretical and experimental results show that, for the presented system, the calibration curves have the following characteristics:

- after first conditioning – the super-Nernstian response,
- after the second – Nernstian response with lower detection limit,
- and after the third – Nernstian response with higher detection limit.

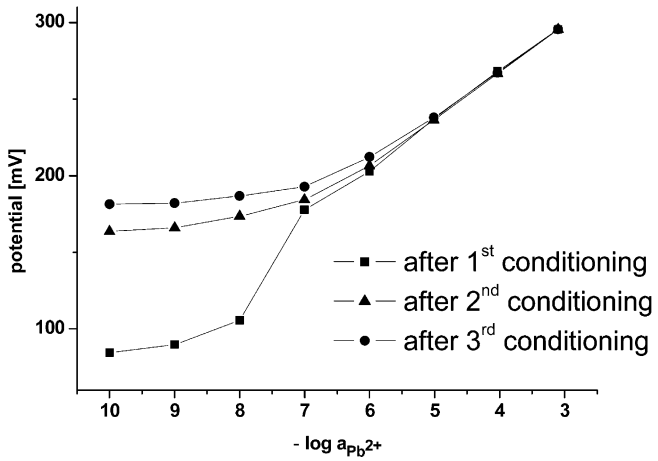

Fig. 6. Experimental response of SC Pb^{2+}-ISE.

The detection limit obtained in the experiment corresponds well with the one obtained from the simulations. The super-Nernstian jump is smaller than the one obtained from the calculations. The difference between the experiment and calculations is caused by the fact that many of the parameters of the system are unknown, and the values used in the numerical experiments are estimated. Because the parameters are inter-connected, it is very difficult and time-consuming to find the proper/optimal set of parameters by trial and error method. The quantitative agreement can be obtained by using the stochastic methods to search for the optimal parameters. One of such method, namely Hierarchical Genetic Strategy (HGS), has been already combined with the NPP model and presented in [37,38].

4 Conclusions

All-solid-state ISEs with conducting polymer are analyzed. The theoretical description of the response of all-solid-state electrodes is presented using a multilayer NPP model. The numerical experiments show the enrichment of the polymer matrix with the primary ion. This process is strongly dependent on the time of conditioning.

A lead(II)-selective electrode based on solvent PVC membrane with polybenzopyrene doped with eriochrome black T as intermediate layer was prepared in order to verify the numerical experiment.

A qualitative agreement of the theoretical and experimental results is observed. Both types of these results show the process of enriching the polymer with the main ion, which leads to the changes in the detection limit and slope. This text delivers the first consistent interpretation of the responses of solid-contact ion-selective electrodes with polymer membranes.

Acknowledgements

Graduate School of Chemical Engineering is acknowledged for financial support.

References

[1] J. Bobacka, A. Ivaska, A. Lewenstam, *Chem. Rev.* **2008**, *108*, 329.
[2] W. E. Morf, G. Kahr, W. Simon, *Anal. Chem.* **1974**, *46*, 1538.
[3] A. Hulanicki, A. Lewenstam, *Talanta* **1976**, *23*, 661.
[4] A. Hulanicki, A. Lewenstam, M. Maj-Żurawska, *Anal. Chim. Acta* **1979**, *107*, 121.
[5] T. Sokalski, A. Ceresa, T. Zwickl, E. Pretsch, *J. Am. Chem. Soc.* **1997**, *119*, 11347.
[6] E. Pretsch, *Trends Anal. Chem.* **2007**, *26*, 46.
[7] A. Konopka, T. Sokalski, A. Michalska, A. Lewenstam, M. Maj-Zurawska, *Anal. Chem.* **2004**, *76*, 6410.
[8] A. Michalska, K. Maksymiuk, *Anal. Chim. Acta* **2004**, *523*, 97.
[9] S. Anastasova-Ivanova, U. Mattinen, A. Radu, J. Bobacka, A. Lewenstam, J. Migdalski, M. Danielewski, D. Diamond, *Sens. Actuators B* **2010**, *146*, 199.
[10] S. Yu, F. Li, W. Qin, *Sens. Actuators B* **2011**, *155*, 919.
[11] A. Cadogan, Z. Gao, A. Lewenstam, A. Ivaska, D. Diamond, *Anal. Chem.* **1992**, *64*, 2496.
[12] A. Lewenstam A, J. Bobacka, A. Ivaska, *J. Electroanal. Chem.* **1994**, *368*, 23.
[13] J. Bobacka, A. Ivaska, A. Lewenstam, *J. Electroanal. Chem.* **1994**, *368*, 33.
[14] T. Blaz, J. Migdalski, A. Lewenstam, *Talanta* **2000**, *52*, 319.
[15] J. Bobacka, *Electroanalysis* **2006**, *18*, 7.
[16] E. Bakker, E. Pretsch, *Trends Anal. Chem.* **2005**, *24*, 199.
[17] Ch. M. McGraw, T. Radu, A. Radu, D. Diamond, *Electroanalysis* **2008**, *20*, 340.
[18] G. Lisak, T. Sokalski, J. Bobacka, L. Harju, A. Lewenstam, *Talanta* **2010**, *83*, 436.
[19] G. Lisak, T. Sokalski, J. Bobacka, L. Harju, K. Mikhelson, A. Lewenstam, *Anal. Chim. Acta* **2011**, *707*, 1.
[20] T. R. Brumleve and R. P. Buck, *J. Electroanal. Chem.* **1978**, *90*, 1.
[21] T. Sokalski, A. Lewenstam, *Electrochem. Commun.* **2001**, *3*, 107.
[22] T. Sokalski, P. Lingenfelter, A. Lewenstam, *J. Phys. Chem. B* **2003**, *107*, 2443.
[23] P. Lingenfelter, I. Bedlechowicz-Sliwakowska, T. Sokalski, M. Maj-Zurawska, A. Lewenstam, *Anal. Chem.* **2006**, *78*, 6783.
[24] T. Sokalski, W. Kucza, M. Danielewski, A. Lewenstam, *Anal. Chem.* **2009**, *81*, 5016.
[25] R. Filipek, *Polish Ceramic Bull.* **2005**, *90*, 103.
[26] J. J. Jasielec, T. Sokalski, R. Filipek, A. Lewenstam, *Electrochim. Acta* **2010**, *55*, 6836.
[27] A. Lewenstam, *J. Solid State Electrochem.* **2011**, *15*, 15.
[28] J. Jasielec, *Master Thesis AGH-UST/ÅAU* **2008**, (http://users.abo.fi/jjasiele/pliki/thesis.pdf)
[29] W. Kucza, M. Danielewski, A. Lewenstam, *Electrochem. Commun.* **2006**, *8*, 416.
[30] B. Grysakowski, B. Bozek, M. Danielewski, *Diffus. Defect Data* **2008**, *113*, 273.
[31] L. Y. Heng, K. Toth, E. A.H. Hall, *Talanta* **2004**, *63*, 73.
[32] N. F. Atta, A. Galal, S. M. Ali, *Int. J. Electrochem. Sci.* **2012**, *7*, 785.
[33] G. Lisak, M. Wagner, C. Kvarnström, J. Bobacka, A. Ivaska, A. Lewenstam, *Electroanalysis* **2010**, *22*, 2794.

[34] G. Lisak, J. Bobacka, A. Lewenstam, *J. Solid-State Electrochem.* **2012**, *16*, 2983.
[35] M. Kodoma, C. Sasaki, *Bull. Chem. Soc. Jpn* **1968**, *41*, 127.
[36] P. B. Nikolskii, M. M. Schultz, A. A. Belijustin, *Glass Electrodes for Hydrogen and Other Cations*, (Ed: G. Eisenman) Marcel Dekker, New York **1967**.
[37] J. J. Jasielec, B. Wierzba, B. Grysakowski, T. Sokalski, M. Danielewski, A. Lewenstam, *ECS Trans.* **2011**, *33*, 19.
[38] B. Grysakowski, J. J. Jasielec, B. Wierzba, T. Sokalski, A. Lewenstam, M. Danielewski, *J. Electroanal. Chem.* **2011**, *662*, 143.

